Use of WLF-like Function for Describing the Nonlinear Phase Separation Behavior of Binary Polymer Blends

Qiang Zheng,* Mao Peng, Yihu Song, and Tiejun Zhao

Department of Polymer Science and Engineering, Zhejiang University, 310027, Hangzhou, China

Received July 25, 2000; Revised Manuscript Received March 27, 2001

ABSTRACT: The spinodal decomposition (SD) of poly(methyl methacrylate)/poly(styrene-*co*-acrylonitrile) (PMMA/SAN) blends is investigated by the time-resolved small-angle light scattering (SALS) technique. It is found experimentally that the evolution of scattering intensity follows the time−temperature superposition principle. The time-dependent scattering intensity $I(t)$ and the temperature-dependent apparent diffusion coefficient $D_{app}(T)$ can be described by the WLF-like function. It is also found that the SD behavior of polystyrene/poly(methyl methacrylate-*stat*-cyclohexyl methacrylate) (PS/PMsC) investigated by other researchers also follows the time−temperature superposition principle.

1. Introduction

Morphology evolution driven by the thermally induced phase separation of low critical solution temperature (LCST) type polymer blends has attracted extensive attention for about two decades due to its great significance to optimizing the mechanical properties of multicomponent/multiphase polymers. Many systems have been studied, such as polystyrene (PS)/poly(vinyl methyl ether) (PVME),[1−4] poly(methyl methacrylate) (PMMA)/poly(styrene-*co*-acrylonitrile) (SAN),[5−8] polycarbonate (PC)/poly(methyl methacrylate) (PMMA),[9−13] SAN/poly(maleic anhydride-*co*-styrene) (SMA),[14] PS/poly(methyl methacrylate-*stat*-cyclohexyl methacrylate) (PMsC),[15] low molecular weight PS/poly(methylphenylsiloxane) (PMPS),[16,17] and PS/polybutadiene (PB).[18,19]

Small-angle light scattering (SALS) is a powerful technique to the study of phase separation behavior of polymer blends, because of its ability to determine the weak concentration fluctuation and fine domain size at the very early stage of phase separation, provided the polymer pair differ enough in refractive index.[15,20]

It has been found that LCST-type polymer blends usually follow the spinodal decomposition (SD) mechanism at temperatures above the critical temperature. The linearized theory introduced by Cahn and Hiliard for explaining the early stage SD of micromolecule system has been proved experimentally to be suitable for polymeric systems, too. Hashimoto[2] found that the temperature-dependent apparent diffusion coefficient $D_{app}(T)$ exhibits a linear relationship with temperature approaching the equilibrium SD temperature T_s for PS/PVME, and T_s can be obtained by extrapolating $D_{app}(T)$ to zero. Snyder[3] also confirmed the linear temperature dependence of $D_{app}(T)$ for PS/PVME.

However, this linear principle is invalid for deep temperature quenches, namely large $(T - T_s)$ value, as is reported by Kyu[10] and Edel[15] for PC/PMMA and PS/PMsC blends, respectively. It was found that the temperature dependence of $D_{app}(T)$ is nonlinear in the temperature region investigated. The $D_{app}(T)$ values increase nearly exponentially with temperature over the investigated temperature region, and it is impossible to obtain the equilibrium spinodal temperature by linear extrapolation even for the data at relatively low temperatures. This means that the temperatures investigated in their experiments are much far from the equilibrium spinodal temperature, and the phase separation occurs in the diffusion-controlled region. Phase separation behavior under considerably lower temperatures was not performed due to some inconvenience, for example, the thermal degradation of polymer in prolonged isothermal annealing.

It has been well accepted that the relaxation time of amorphous polymers controlled by diffusion of segments obeys the time−temperature superposition (TTS) principle and can be described by the Williams−Landel−Ferry (WLF) function in the glass transition region.[21] Furthermore, the temperature dependence of segment diffusion and diffusion-controlled reaction in polymer systems can also be described by the WLF function.[22,23] For the phase separation of polymer blends, the growth rate of new phase domains depends strongly on the diffusivity of macromolecular chains. In view of the great success of TTS principle to the noncritical polymer diffusion, we want to know whether the phase separation behavior of binary polymer blends at deep temperature quenches also follows the TTS principle or not. Up to date, just few researchers have dealt with this topic. Maruta et al.[14] had noticed that at late stage of SD $\log I(q_m)$−$\log t$ and $\log q_m$−$\log t$ plots at different temperatures can be reduced to a master curve by horizontal and vertical shifting for SAN/SMA blends, indicating the applicability of TTS.

In this paper, the binary blends of poly(methyl methacrylate)/poly(styrene-*co*-acrylonitrile) (PMMA/SAN) exhibiting LCST behavior and appropriate temperature region for the experiment are selected as a model system. The evolution of scattering intensity and the temperature dependence of $D_{app}(T)$ during isothermal annealing are investigated. Taking into account that the miscibility, phase separation mechanism, and kinetics of PMMA/SAN blends have been extensively studied by McMaster,[5] Kammer,[6] Nishimoto,[7] and Maruta[8] et al., we focus our attention on the nonlinear phase separation behavior over a wide temperature region. We will try to explore the possibility of application of TTS principle and WLF function to describe the evolution of scattering intensity and the relationship between D_{app}-

* To whom correspondence should be addressed. E-mail: ipczju@cmsce.zju.edu.cn.

10.1021/ma0013105 CCC: $20.00 © 2001 American Chemical Society
Published on Web 10/18/2001

(T) and isothermal annealing temperature for PMMA/SAN.

2. Experimental Section

2.1. Materials. Commercial available poly(methyl methacrylate) (PMMA) ($M_n = 8 \times 10^4$, $M_w/M_n = 2.1$) and poly(styrene-*co*-ancrylonitrile) (SAN) ($M_n = 4.5 \times 10^4$, $M_w/M_n = 2.2$, Chimei Co., Ltd., Taiwan) with AN content of 32 wt % were employed in this study. The PMMA/SAN (60 wt/40 wt) films for SALS observation were prepared by dissolving the polymers in dichloromethane (CH_2Cl_2) at a weight fraction of 20%, and then solvent casting on the surface of microscope slides preheated to 32 °C. After the solvent evaporated at ambient environment, the samples were further dried at 80−90 °C in a vacuum oven for at least 24 h to ensure that no residual solvent existed. The resultant samples with thickness of about 40 μm were homogeneous and transparent. No detectable phase separation can be observed by using either an optical microscope or SALS.

2.2. Dynamic Rheological Measurements. ARES (Rheometric Scientific) was employed to measure the glass transition temperature of PMMA/SAN blends. Several PMMA/SAN films with thickness of about 100 μm obtained by using the methods mentioned above were overlaid and prepared into rectangular samples with length, width, and thickness of 30.0, 12.5, and 0.8 mm, respectively, by hot pressing at 130 °C and 5 MPa. The procedure of press molding was performed within 5 min in order to diminish the influence of heating on the phase morphology as far as possible. The heating rate and the frequency used dynamic rheological measurements were 2 °C min^{-1} and 10 rad s^{-1}, respectively.

2.3. Time-Resolved Small-Angle Light Scattering (SALS). A time-resolved SALS apparatus similar to that described in many earlier papers[2,4,7] was used in this work. The gray scale images of the scattering patterns with resolution of 540 × 660 × 24 bits were captured in real time by a CCD digital camera (MTV-1802CB, MINTRON, Taiwan) and then imported into the computer memory at the minimum time interval of 2 s through a video capturing board (VIDEO VESA, Daheng, Beijing). Online circular averaging of each radius symmetric scattering pattern was performed to obtain the intensity distribution, namely the relationship between intensity and scattering angle. The intensity at the beginning of examination was subtracted from the intensity measured at later time as background to avoid the negative effects of parasitic light, thermal fluctuation in the homogeneous samples, and the dark current of CCD camera. The recording intervals can be altered at the beginning of the experiment according to different phase separation speed, which is determined by the experimental temperature and the compositions of the samples. The images can also be auto-saved as bitmap files with the size of 1200 kbytes. For isothermal annealing experiment, the hot stage with power of 100 W and controlled by an intelligent controller (AI-700, YUGUANG, Xiamen) was preheated to the appointed temperatures before the samples were placed on. The overheating of the hot stage after the sample being placed on was limited to about 0.5 °C by the controller. The temperature usually reached equilibrium within 10−40 s after the samples were placed on, depending on the temperature of the hot stage. For all the isothermal experimental temperatures in this paper, the time for temperature recovery is negligible as compared with the entire experimental time. The accuracy of temperature control was on the order of ±0.2 °C.

3. Theoretical Background

3.1. Early Stage of Spinodal Decomposition. The linear theory from Cahn and Hilliard can be used to describe the intensity evolution at the initial stage of phase separation of binary polymer blends.[24] Considering the thermal fluctuation of stable binary polymer blends, Cook modified the Cahn−Hilliard function into[25]

$$I(q,t) = I_s(q,0) + (I(q,0) - I_s(q,0)) \exp(2R(q)t) \quad \text{(III-1)}$$

in which $I_s(q,0)$ is the scattering intensity of the stable system. The relaxation rate or amplification factor, $R(q)$, is further related by

$$R(q) = -Mq^2\left(\frac{\partial^2 f_m}{\partial \phi^2} + 2\kappa q^2\right) \quad \text{(III-2)}$$

Here M, ϕ, κ, and f_m are the mobility (assumed to be q-independent), the volume fraction of component B, the gradient energy coefficient, and the mean field free energy of mixing, respectively.

Equation III-2 includes the apparent diffusion coefficient D_{app}, which describes the uphill diffusion during spinodal decomposition

$$D_{app} = -M\frac{\partial^2 f_m}{\partial \phi^2} \quad \text{(III-3)}$$

From eq III-1 one can find that plots of $\ln(I(q,t) - I_s(q,0))$ vs t yields $R(q)$, and then from eqs III-2 and III-3 one can obtain the D_{app} and $2M\kappa$ values from the intercept and slope of the plot of $R(q)/q^2$ vs q^2.

3.2. Late Stage of Spinodal Decomposition. At the late stage of SD, the concentration fluctuation approaches the value equal to the coexisting curve, while the phase domains keep on changing in both size and shape in order to reduce the interface.[15] This coarsening process follows the power laws, in which the evolution of q_m and $I(q_m)$ at the late stage is described as

$$I(q_m(t)) \propto t^{\beta} \quad \text{(III-4)}$$

$$q_m(t) \propto t^{\alpha} \quad \text{(III-5)}$$

According to the theory of Siggia,[26] for most polymer−polymer binary blends, the relationship between exponents α and β follows $\beta = 3\alpha$.

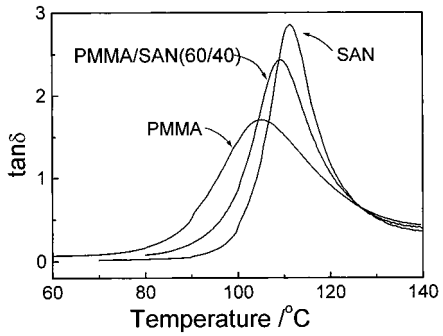

Figure 1. Temperature dispersion curves of loss tangent (tan δ) for pure PMMA, SAN, and PMMA/SAN(60/40) blends.

4. Results and Discussion

4.1. Glass Transition Temperature (T_g). Figure 1 presents the temperature dispersion curves of loss tangent (tan δ) for pure PMMA, SAN, and PMMA/SAN (60/40) blend. It was found that the glass transition temperature (T_g) of pure PMMA, pure SAN, and PMMA/

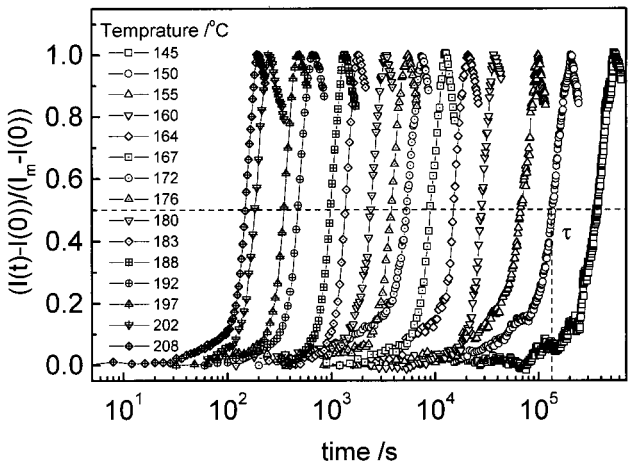

Figure 2. Time evolution of normalized scattering intensity of PMMA/SAN (60/40) blends at $q = 6.5\ \mu m^{-1}$ under different annealing temperatures.

SAN (60/40) blend are 105.5, 111.4, and 109.4 °C, respectively. Only a single T_g for PMMA/SAN(60/40) blends can be observed. The experimental T_g value is somewhat higher than the theoretical value 107.8 °C, obtained from the Fox equation[27]

$$1/T_g = w_A/T_{g,A} + w_B/T_{g,B} \qquad \text{(IV-1)}$$

in which w is the weight fraction of the component and subscripts of A and B represent the two components of polymer blends, respectively. This positive deviation is coincided with the results reported by Wu.[28] As only a single T_g for PMMA/SAN (60/40) blends was obtained, it can be believed that there exists single phase in this blends films prepared by solvent casting. Usually, the reference temperature of WLF function is selected as 50 °C higher than T_g, due to the proper relaxation time at this temperature. Hence, in this paper, 160 °C, which is about 50 °C higher than T_g of the PMMA/SAN (60/40) blends, is selected as the reference temperature of the WLF function in the later discussion.

4.2. Evolution of Intensity *I*(*t*) during Isothermal Process. To avoid the negative effect of the sample diversity resulted from concentration inhomogeneity and difference of thickness for various samples, the scattering intensity at given scattering vector, $I(t)$, is normalized as $(I(t) - I(0))/(I_m) - I(0))$, in which $I(0)$ is the intensity at the start of experiment and I_m is the maximum value of $I(t)$ during thermal annealing. Figure 2 presents the semilogarithmic plots of $(I(t) - I(0))/(I_m - I(0))$ vs time at $q = 6.5\ \mu m^{-1}$ of isothermal annealing under different temperatures. It is very interesting that all curves for different temperatures are nearly parallel to each other, indicating that they can superpose with each other and then form a master curve by horizontal shifting. This means that the TTS principle is applicable in this case.

When setting 160 °C as the reference temperature T_r, the logarithmic shifting factor $\log \alpha_T = \log(\tau/\tau_r)$ can be calculated according to Figure 2, here τ_r is the relaxation time at T_r and τ is the relaxation time at which the normalized scattering intensity for different temperatures increases by the same degree, as is shown for example 50% in Figure 2. Figure 3 gives the plots of α_T against temperature. It is noted that α_T obtained here decreases exponentially with temperature, similarly to that of the well-known viscoelastic behavior that follows

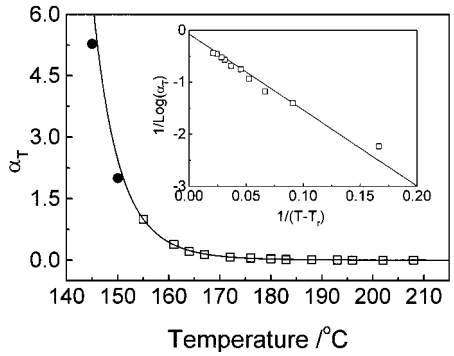

Figure 3. Relationship between shifting factor α_T and temperature for PMMA/SAN (60/40) blends at $q = 6.5\ \mu m^{-1}$.

the TTS principle. The inlay of Figure 3 gives the plots of $1/\log \alpha_T$ against $1/(T - T_r)$, exhibiting perfect linear relationship. Hence, we can obtain the WLF-like function

$$\log \alpha_T = \log \frac{\tau}{\tau_r} = \frac{-C_1(T - T_r)}{C_2 + T - T_r} \qquad \text{(IV-2)}$$

with the constants $C_1 = 8.76$ and $C_2 = 135.8$ °C. The data error for C_1 and C_2 are about 20%. It is interesting that the C_1 and C_2 values are considerably close to the empirical constants of 8.86 and 101.6 in the universal WLF function for polymer melts viscosity, where the reference temperature is usually selected about 50 °C higher than T_g. This indicates the fact that the phase separation behavior of PMMA/SAN blends also follows the TTS principle. After investigating the time evolution of scattering intensity at several vectors within the region from 1.0 to 6.8 μm^{-1}, we can conclude that eq IV-2 is also valid for all scattering vectors in the observation region with nearly the same values of C_1 and C_2.

The relaxation time τ over a very wide temperature region is calculated by using eq IV-2, as presented by the curve in Figure 3. It is found that τ increases rapidly with temperature decrease. Even at temperature adjacent to T_g of PMMA/SAN blends, phase separation is still possible to be observed if observation time can be prolonged to long time enough, such as several years. Apparently, this is too long to be realized. But fortunately, it is possible to observe phase separation within the temperature region from 140 to 155 °C in the period of 1 week. To confirm the reliability of eq IV-2, we conducted isothermal annealing experiments at 155, 150, and 145 °C. As predicted, remarkable phase separation was finally detected after several days thermal treatment. For 145 °C, 1 week is required for the full phase separation process. It should be emphasized that phase separation occurred in the temperature region from 145 to 155 °C can be proved to follow the SD mechanism, which will be discussed in the next section. As shown by the solid points in Figure 3, the shifting factors obtained experimentally for 155, 150, and 145 °C are in correspondence with the calculating result well, meaning that function (IV-2) at least is applicable at temperatures higher than 145 °C. It should be pointed out that no discernible thermal degradation and oxidization of PMMA or SAN occurred during the long-term observation under all the experimental temperatures.

As reported in the literature,[6,8] the spinodal curve of PMMA/SAN blends are 30−80 °C higher than the T_g−

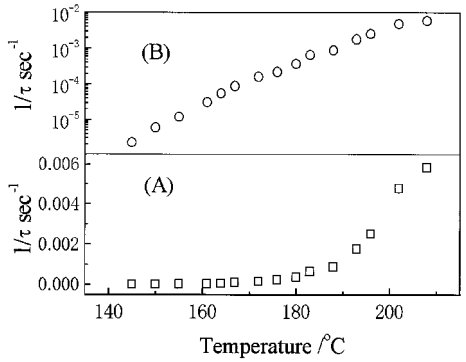

Figure 4. Calculated relaxation time τ as the function of temperature.

composition curve, depending on the composition, the molecular weight, and AN content of SAN copolymer. The spinodal curve is also obtained by long time isothermal annealing, for example 48 h. However, as mentioned above, 1 week is necessary to observe the phase separation at 145 °C for the PMMA/SAN blends studied here. Therefore, it is impossible to obtain the equilibrium phase diagram of the present PMMA/SAN blends from isothermal annealing within a limited period of time. Strictly speaking, at critical SD temperature τ should be infinite. Parts A and B of Figure 4 present the plot and semilogarithm plot of $1/\tau$ against temperature, respectively. Because of the exponential relationship between $1/\tau$ and temperature for the three points at 145, 150, and 150 °C, as can be seen in Figure 4B, it is impossible to obtain the equilibrium SD temperature by linearly extrapolating $1/\tau$ into zero. Therefore, 145 °C should be much higher than the critical SD temperature of the present PMMA/SAN blends. From eq IV-2, one can find that τ approaches infinite when the experimental temperature approaches $(T_r - C_2)$, suggesting that the equilibrium SD temperature may be $(T_r - C_2)$, about 80 °C lower than the T_g in the present system. Unfortunately, phase separation would not be experimentally observed under T_g due to the freezing of macromolecular chains. Some other system, for example the SAN (with 25% AN in copolymer)/SMA system, also has a critical temperature lower than glass transition temperature over certain composition, as is reported by Maruta.[14]

It can be found from Figure 4 that τ of PMMA/SAN (60/40) jumps to several hundred hours when the temperature approaches 130 °C, meaning that detectable phase separation cannot be observed within limited period of time. As mentioned above, the time for preparing PMMA/SAN (60/40) samples by press-molding at 130 °C for dynamical measurements was 5 min, which is entirely negligible as compared with τ.

4.3. Early Stage of Spinodal Decomposition. In view of practical applications, the morphology evolution of polymer blends can be predicted and controlled, in case the phase separation kinetics has been understood. For example, Kyu[13] obtained the bicontinuous phase morphology of PC/PMMA by using the SD method at appropriate processing temperature and time. It was found that the bicontinuous morphology with the characteristic of interpenetrating polymer networks (IPNs) can be contributed to the mechanical modification of PC/PMMA, especially the toughness, due to the improved interfacial properties. However, phase separation at relatively low temperatures was not investigated enough

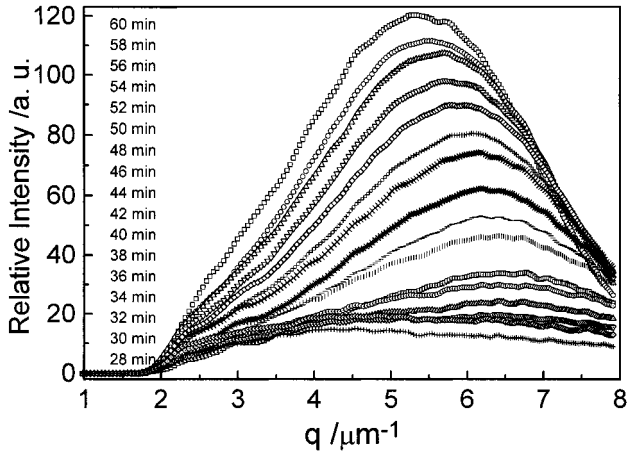

Figure 5. Intensity profiles of PMMA/SAN (60/40) blends at 183 °C.

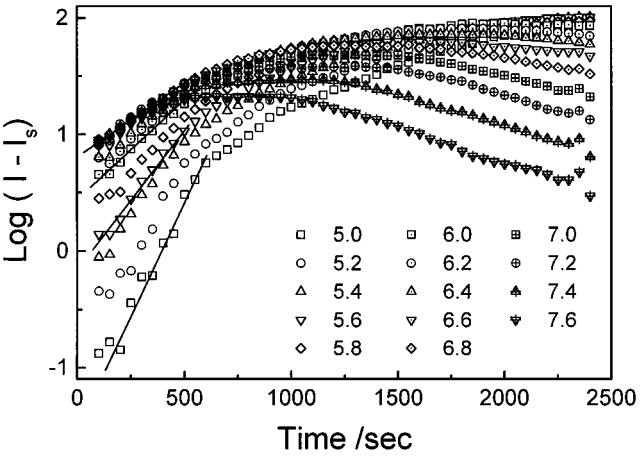

Figure 6. Time evolution of $\log(I - I_s)$ of PMMA/SAN (60/40) blends for various scattering vectors at 183 °C.

to date due to the inconvenience of long-term experiments. Here we study the phase separation kinetics of PMMA/SAN (60/40) on the basis of linearized Cahn–Hilliard theory over a wide temperature region and believe the phase separation behavior of PMMA/SAN blends at lower temperatures may be predicted when the influence of temperature is illuminated.

Figure 5 gives the evolution of intensity profiles during the phase separation process at 183 °C. The scattering vector with maximum scattering intensity, q_m, appears constant at the early stage and then decreases with time, while the relative intensity of scattered light increases continually from the beginning of the test. It is noticed that there exhibit the same characteristics at all the temperatures investigated, including relatively low temperatures such as 145, 150, and 155 °C. This indicates that PMMA/SAN blends show typical spinodal decomposition behavior over the temperature region.

The typical plots of $\log(I - I_s)$ vs time for different scattering vectors q from 5.0 to 7.6 μm^{-1} at 183 °C are shown in Figure 6. In correspondence with the linearized Cahn–Hilliard theory, the time dependence of $\log(I - I_s)$ is satisfactorily linear at the early stage of SD.

According to eq III-1, $R(q)$ values can be obtained from the slopes of the initial segment of $\log(I - I_s)$–t curves for various vectors in Figure 6. Furthermore, $D_{app}(T)$

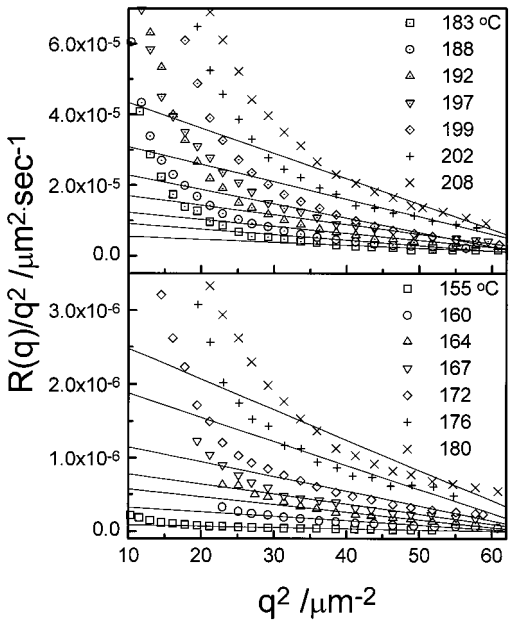

Figure 7. Relationship between $R(q)/q^2$ and q^2 for PMMA/SAN (60/40) blends at various temperatures.

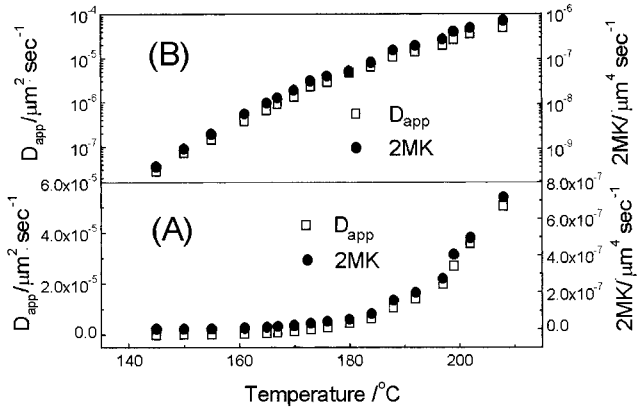

Figure 8. (A) Temperature dependence of $D_{app}(T)$ and $2M\kappa(T)$ and (B) semilogarithmic curve of temperature dependence of $D_{app}(T)$ and $2M\kappa(T)$ for PMMA/SAN (60/40) blends.

and $2M\kappa$ for different temperatures can be obtained from intercepts and slopes of $R(q)/q^2-q^2$ curves as shown in Figure 7. $R(q)/q^2$ vs q^2 in present system follows linear relationship well at large q values. The linear function is invalid for small q values. Figure 8A presents the $D_{app}(T)$ and $2M\kappa$ values as a function of temperature. Figure 8B presents the semilogarithmic plot of $D_{app}(T)$ and $2M\kappa$ against temperature. It is found that neither $D_{app}(T)$ nor $2M\kappa$ is a linear function of temperature, and it is impossible to obtain the critical SD temperature by linear extrapolation $D_{app}(T)$ or $2M\kappa$ to zero. Because phase separation of PMMA/SAN follows SD mechanism over the whole temperature region investigated, the nonlinear function of $D_{app}(T)$ or $2M\kappa$ against temperature is not resulted from the change of phase separation mechanism from SD to nuclear and growth (NG) mode as temperature decreasing.

The linear functions for $1/\log(D_{app}(T_r)/D_{app}(T))-1/(T - T_r)$ and $1/\log(2M\kappa(T_r)/2M\kappa(T))-1/(T - T_r)$ using 160 °C as the reference temperature as shown in the inlays of Figure 9A,B indicate that the WLF-like function is also applicable to describe the temperature dependence of $D_{app}(T)$ and $2M\kappa$. The constants in WLF-like functions obtained from the interceptions and slops of the above

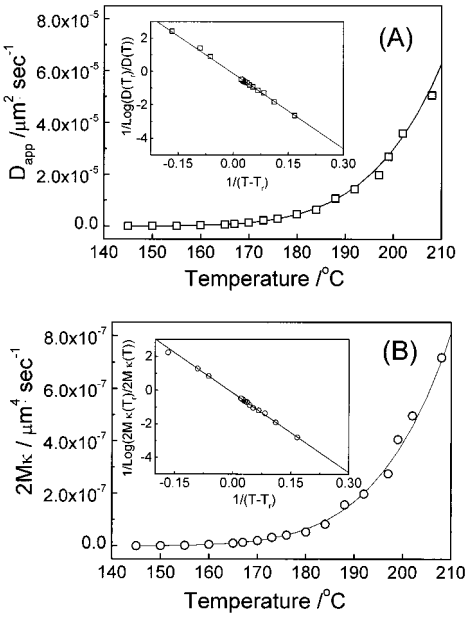

Figure 9. Temperature dependence of (A) $D_{app}(T)$ and (B) $2M\kappa(T)$ for PMMA/SAN (60/40) blends. The inlays present the $1/\log(D_{app}(T_r)/D_{app}(T))-1/(T - T_r)$ and $1/\log(2M\kappa(T_r)/2M\kappa(T))-1/(T - T_r)$ relation at the reference temperature 165 °C.

two linear functions are $C_1 = 6.69$, $C_2 = 99.28$ °C and $C_1 = 6.81$, $C_2 = 107.81$ °C, respectively. Then, we obtain

$$\log \frac{D_{app}(T_r)}{D_{app}(T)} = \frac{-C_1(T - T_r)}{C_2 + T - T_r} \qquad \text{(IV-3)}$$

$$\log \frac{M\kappa(T_r)}{M\kappa(T)} = \frac{-C_1(T - T_r)}{C_2 + T - T_r} \qquad \text{(IV-4)}$$

The data error for C_1 and C_2 are estimated to be about 20%. The empirical constants for $D_{app}(T)$ and $2M\kappa$ in the WLF-like function can be regarded as the same. Thus, we can substitute eqs IV-3 and IV-4 into eq III-2, and then $R(q)$ can be related to temperature by

$$\log \frac{R(T_r)}{R(T)}|_q = \frac{-C_1(T - T_r)}{C_2 + T - T_r} \qquad \text{(IV-5)}$$

By averaging the values of C_1 and C_2 in eqs IV-3 and IV-4, $C_1 = 6.75$ and $C_2 = 103.5$ °C are obtained for eq IV-5.

To validate eq IV-5, the $R(q)/q^2$ values under $q = 6.0$ μm^{-1} for various temperatures are extracted from the $R(q)/q^2$ vs q^2 plots in Figure 7, and $R(q)$ is then plotted against temperature as shown in Figure 10. It can be found that the temperature dependence of $R(T)$ is also typically nonlinear. When selecting 160 °C as the reference temperature, $1/\log(R(T_r)/R(T))$ vs $1/(T - T_r)$ is found to follow the linear principle given by eq IV-5. By using least-squares fitting, the C_1 and C_2 values are estimated as 6.7 and 101.5 °C, respectively, which are very close to the calculated values.

It is worth noticing that the C_1 and C_2 values in eq IV-5 are roughly equal to those in eq IV-2 within the error region. Through comparing eq IV-5 with eq IV-2, we can find that τ for certain q is proportional to the inversion of $R(T)$ under the same q. This indicates that there must exist intrinsic relationships between these two parameters. By introducing eq III-1, we can trans-

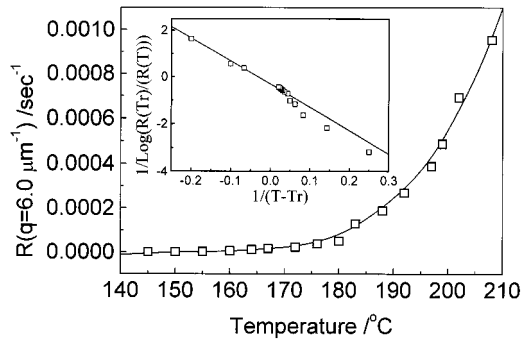

Figure 10. Temperature dependence of relaxation rate $R(T)$ at scattering vector of 6.0 μm^{-1} for PMMA/SAN (60/40) blends. The inlays present the $1/\log(R(T_r)/R(T))-1/(T - T_r)$ relation at the reference temperature 165 °C.

form the normalized intensity in section 4.2 into following equation

$$\frac{I(t) - I_s(0)}{I_m - I_s(0)} = \frac{I(0) - I_s(0)}{I_m - I_s(0)} \exp\{2R(T)t\} = A \exp\{Bt/\tau\} \quad \text{(IV-6)}$$

where A and B are constants dependent on the scattering angle. It is very interesting that eq IV-6 has the same form of the relaxation equation suitable to most polymeric materials, $\Delta x(t) = \Delta x_0 e^{-t/\tau}$, in which $\Delta x(t)$ is the length increasement of the fiber sample at time t, Δx_0 is the length increase at the beginning of the experiment, and τ is the relaxation time which also follows the WLF function.[29] The similarity of the two phenomena indicates that the intensity evolution induced by phase separation is also a relaxation behavior controlled by the movement of macromolecule segments.

The slow phase separation during isothermal annealing at relatively low temperatures is associated with the polydispersity of molecular weight and the heterogeneities of the sequence statistic for the random copolymers due to their great significance to phase separation behavior. But the effect of relaxation behavior of macromolecular chains has been seldom taken into consideration. It is well-known that at the early stage SD proceeds by the diffusional flux against the concentration gradient and the growth rate of new phase domains depends strongly on the diffusivity of macromolecular chains. Thereby, it is believed that the slow phase separation rate in PMMA/SAN is due to the poor mobility of molecules and the high viscosity of the matrix at relatively low temperature.

When applying the WLF-like function to examine the temperature dependence of $D_{app}(T)$ and $2M\kappa$ for PS/PMsC system obtained by Edel,[7] as presented in Figure 11A,B, we can obtain the satisfactory linearity function of $1/\log(D_{app}(T_r)/D_{app}(T))-1/(T - T_r)$ and $1/\log(2M\kappa(T_r)/2M\kappa(T))-1/(T - T_r)$ using 165 °C as the reference temperature, as shown in the inlays. The results similar to that of PMMA/SAN system indicate that the TTS principle is also applicable for the PS/PMsC system. The WLF empirical constants obtained here are $C_1 = 9.87$, $C_2 = 48.93$ °C for $1/\log(D_{app}(T_r)/D_{app}(T))-1/(T - T_r)$ curve and $C_1 = 13.68$, $C_2 = 53.54$ °C for $1/\log(2M\kappa(T_r)/2M\kappa(T))-1/(T - T_r)$ curve. It is suggested that the difference of parameters C_1 and C_2 of PS/PMsC with those of PMMA/SAN is resulted from the difference in chemical structure of two systems.

As reported by Hashimoto,[2] Snyder,[3] and Parizel[4] et al., PS/PVME blends show a nearly linear $D_{app}(T)-T$ relationship over the investigated temperature region. This is in marked contrast to the exponential WLF behavior of PMMA/SAN, and PS/PMsC as is shown above. As Maruta[14] pointed out, phase separation rate and chain mobility in PS/PVME blends are much higher and less sensitive to the increase of temperature than those in some other polymer blends of higher viscosity, such as poly(maleic anhydride-*co*-styrene)/poly(anhydride-*co*-styrene) (SMA/SAN). This indicates that diffusion and viscosity play more important roles in those systems showing slower phase separation rate than that in PS/PVME.

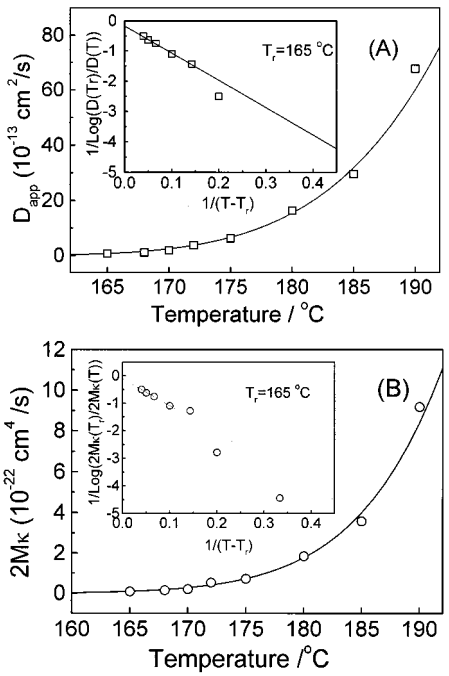

Figure 11. Temperature dependence of (A) $D_{app}(T)$ and (B) $2M\kappa(T)$ for PS/PMsC blends. The inlays present the $1/\log(D_{app}(T_r)/D_{app}(T))-1/(T - T_r)$ and $1/\log(2M\kappa(T_r)/2M\kappa(T))-1/(T - T_r)$ relation at reference temperature 165 °C.

4.4. Late Stage of Spinodal Decomposition. Other than that at the early stage SD, the concentration fluctuation at the late stage SD approaches saturation. The strengthening of scattered intensity and the shifting of maximum scattering vector to smaller values are mainly resulted from coarsening of new phase domains. Siggia[26] revealed that the coarsening of phase domains at the late stage SD occurs through the percolation process in which the melts diffuse via interconnected channels driven by interface tension. According to his calculation, the slope of the log $I(q_m)$−log t plot, α, and the slope of the log q_m−log t plot, β, should be 1 and 3, respectively. As described in the literature, perfect linearity for the plots of log $I(q_m)$−log t and log q_m−log t at various temperatures can be obtained. Similar plots in Figure 12A,B for PMMA/SAN (60/40) blends indicate that the power laws are also applicable to describe the character of late stage SD for these blends. The values of α and β, for all the temperatures investigated, are about 0.9 and 2.8, respectively, practically equal to the values suggested by Siggia.[26]

As mentioned above, Maruta et al.[14] had noticed that log $I(q_m)$−log t and log q_m−log t plots at different temperatures can be reduced to a master curve by horizontal and vertical shifting for SAN/SMA blends. The fact that the log $I(q_m)$−log t plots and log q_m−log t plots are parallel with each other suggests that they can

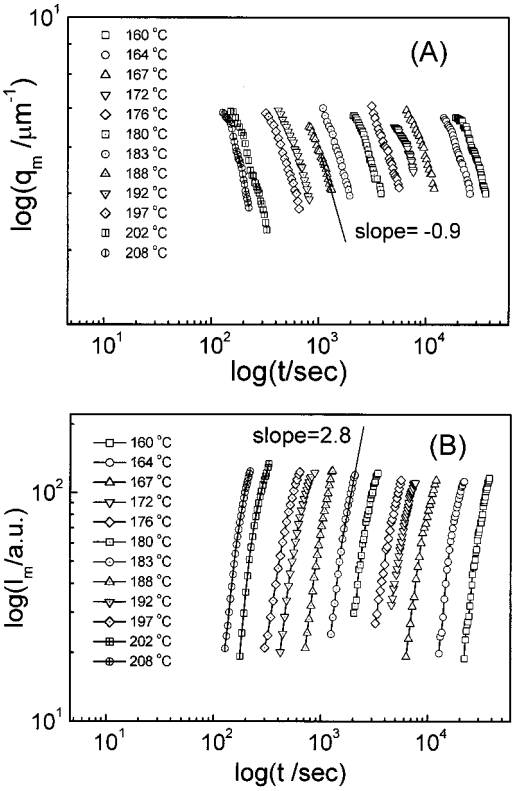

Figure 12. (A) Time evolution of q_m and (B) time evolution of I_m for PMMA/SAN(60/40) blends at late stage SD under various temperatures.

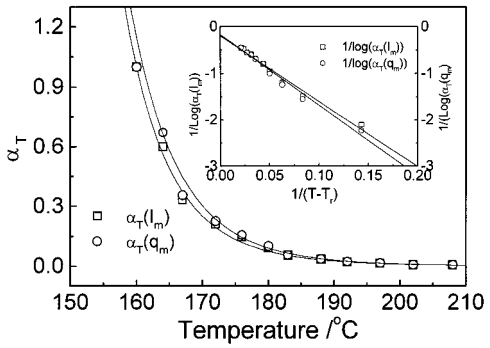

Figure 13. Plots of $1/\log(\alpha(I_m))-1/(T - T_s)$ and $1/\log(\alpha(q_m))-1/(T - T_s)$ at late stage SD for PMMA/SAN (60/40) blends.

be superposed to form a respective master curve by horizontal shifting. TTS principle is thus applicable. The shifting factors for $I(q_m)$ and q_m here are defined as $\alpha(I(q_m)) = \tau(I(q_m))/\tau_r(I(q_m))$ and $\alpha(q_m) = \tau(q_m)/\tau_r(q_m)$, respectively, in which τ is the relaxation time at which $I(q_m)$ for different temperatures increase to the same value and τ_r is the relaxation time of the reference temperature. Figure 13 shows the plots of $1/\log(\alpha(I(q_m)))-1/(T - T_s)$ and $1/\log(\alpha(q_m))-1/(T - T_s)$. The linear results mean that the WLF-like function also fit the relationships satisfactorily. This is understandable since the coarsening process at the late stage SD was mainly controlled by the viscoelastic flow of polymer melts. In the WLF-like function, constants are $C_1 = 8.77$ and $C_2 = 135.9$ °C for $1/\log(\alpha(I(q_m)))-1/(T - T_s)$ and $C_1 = 11.4$ and $C_2 = 188.9$ °C for $1/\log(\alpha(q_m))-1/(T - T_s)$, respectively. They are approximate to the values obtained for the early stage phase separation.

5. Conclusions

The phase separation behavior of PMMA/SAN blends is proved experimentally to follow the time−temperature superposition (TTS) principle within the experimental temperature region. The temperature dependence of apparent diffusion coefficient $D_{app}(T)$ and relaxation time τ of scattering intensity $I(t)$ can be described by the Williams−Landel−Ferry (WLF) function. At temperature approaching T_g, phase separation may occur at a very slow rate due to the very poor mobility of molecular chains and phase separation may be undetectable within the limited observation time. At high temperatures, phase separation may become so fast that it accomplishes before the temperature of the sample approaches the thermal equilibrium. Therefore, application of the TTS principle will afford us valuable information about SD behavior over a much wider temperature region. It will be of practical value in predicting the influence of temperature on the phase behavior of polymer blends during isothermal annealing or melting mixing.

Acknowledgment. We are deeply appreciated to the Special Funds for Major State Basic Research Projects (Grant G1999064800) and the National Nature Science Foundation of China (Grant 59973018) that mainly supported this work. We also thank Mr. Bibo Yang, who afforded kind help in measurements of molecular weight and glass transition temperatures of PMMA/SAN blends. We are also grateful to Prof. Yuliang Yang and Dr. Jiangwen Zhang of Fudan University for their kind help for designing the SALS apparatus.

References and Notes

(1) Nishi, T.; Wang, T. T.; Kwei, T. K. *Macromolecules* **1975**, *8*, 227.
(2) Hashimoto, T.; Kumaki, J.; Kawai, H. *Macromolecules* **1983**, *16*, 641.
(3) Snyder, H. L.; Meakin, P. *Macromolecules* **1983**, *16*, 757.
(4) Parizel, N.; Kempkes, F.; Cirman, C.; Picot, C.; Weill, G. *Polymer* **1998**, *39*, 2.
(5) McMaster, L. P. *Adv. Chem. Ser.* **1975**, *142*, 43.
(6) Suess, M.; Kressler, J.; Kammer, H. W. *Polymer* **1987**, *28*, 957.
(7) Nishimoto, M.; Keskkula, H.; Paul, D. R. *Polymer* **1989**, *30*, 1279.
(8) Maruta, J.; Ohnaga, T.; Inoue, T. *Macromolecules* **1993**, *26*, 6386.
(9) Kyu, T.; Saldanha, J. M. *J. Polym. Sci., Polym. Lett. Ed.* **1988**, *26*, 33.
(10) Kyu T.; Saldanha, J. M. *Macromolecules* **1988**, *21*, 1021.
(11) Lim, D.; Kyu, T. *J. Chem. Phys.* **1990**, *92*, 3944.
(12) Kyu, T.; Lim, D. *J. Chem. Phys.* **1990**, *92*, 3951.
(13) Kyu, T.; Jeanne, M.; Saldanha, M.; Kiesel, J. In *Two-Phase Polymer Systems*; Hanser Publishers: New York, 1991; p 259.
(14) Maruta, J.; Ougizawa, T.; Inoue, T. *Polymer* **1988**, *29*, 2056.
(15) Edel, V. *Macromoleclues* **1995**, *28*, 6219.
(16) Nojima, S.; Nose, T. *Polym. J.* **1982**, *14*, 269.
(17) Nojima, S.; Nose, T. *Polym. J.* **1982**, *14*, 907.
(18) Russell, T. P.; Hadziioannou, G.; Warburton, W. K. *Macromolecules* **1985**, *18*, 78.
(19) Tsai, F. J.; Torkelson, J. M. *Macromolecules* **1988**, *21*, 1026.
(20) Inoue, T. *Prog. Polym. Sci.* **1995**, *20*, 119.
(21) Wisanrakkit, G.; Gillham, J. K. *J. Appl. Polym. Sci.* **1990**, *41*, 2885.
(22) Christopher, W. W.; Cook, W. D.; Goodwin, A. A. *Polymer* **1997**, *38*, 3251.
(23) Kummins, C. A.; Kwei, T. K. In *Diffusion in Polymers*; Crank, J., Park, G. S., Eds.; Academic Press: London, 1968; p 120.
(24) Cahn, J. W. *J. Chem. Phys.* **1965**, *42*, 93.
(25) Cook, H. E. *Acta Metall.* **1970**, *18*, 297.
(26) Siggia, E. D. *Phys. Rev. A* **1979**, *20*, 595.
(27) Fox, T. G. Bull. *Am. Phys. Soc.* **1956**, *1*, 123.
(28) Wu, S. H. *Polymer* **1987**, *28*, 1144.
(29) He, M. J.; Chen, W. X.; Dong, X. X. *Polymer Physics*; Fudan University Publishers: 1997; p 225.
MA0013105